Quality Evaluation of the Column-Averaged Dry Air Mole Fractions of Carbon Dioxide and Methane Observed by GOSAT and GOSAT-2

Yukio Yoshida[1], Yu Someya[1], Hirofumi Ohyama[1], Isamu Morino[1], Tsuneo Matsunaga[1], Nicholas M. Deutscher[2], David W. T. Griffith[2], Frank Hase[3], Laura T. Iraci[4], Rigel Kivi[5], Justus Notholt[6], David F. Pollard[7], Yao Té[8], Voltaire A. Velazco[2, 9], and Debra Wunch[10]

[1]*National Institute for Environmental Studies, Tsukuba, Japan*
[2]*School of Earth, Atmospheric and Life Sciences, Faculty of Science, Medicine and Health, University of Wollongong, Wollongong, NSW, 2522, Australia*
[3]*Karlsruhe Institute of Technology, IMK-ASF, Karlsruhe, Germany*
[4]*NASA Ames Research Center, Moffett Field, California, USA*
[5]*Finnish Meteorological Institute, Sodankylä, Finland*
[6]*Institute of Environmental Physics, University of Bremen, Bremen, Germany*
[7]*National Institute of Water & Atmospheric Research Ltd (NIWA), Lauder, New Zealand*
[8]*Laboratoire d'Études du Rayonnement et de la Matière en Astrophysique et Atmosphères (LERMA-IPSL), Sorbonne Université, CNRS, Observatoire de Paris, PSL Université, 75005 Paris, France*
[9]*Deutscher Wetterdienst (DWD), Meteorological Observatory Hohenpeissenberg, 82383, Germany*
[10]*Department of Physics, University of Toronto, Toronto, Ontario, Canada*

(Manuscript received 10 April 2023, accepted 14 June 2023)

Abstract Column-averaged dry air mole fractions of carbon dioxide and methane (XCO_2 and XCH_4) retrieved from SWIR (Short-Wavelength InfraRed) observations by GOSAT (Greenhouse Gases Observing SATellite) since 2009 and its successor GOSAT-2 since 2019 are available from NIES (National Institute for Environmental Studies) as SWIR L2 (Level 2) products. This paper shows the current status of the data quality of NIES SWIR L2 products and inter-satellite comparison results. Comparisons of XCO_2 and XCH_4 obtained from each satellite with ground-based observations from the TCCON (Total Carbon Column Observing Network) reveal that the averaged single measurement precision are less than 1.9 ppm and 10 ppb, respectively, and the site-to-site biases are less than 0.9 ppm and 5 ppb, respectively. The standard deviations of the inter-satellite differences for XCO_2 and XCH_4 are 2.18 ppm and 12.1 ppb, respectively, on an individual-data basis and 1.77 ppm and 11.7 ppb, respectively, on a monthly-regional-mean basis. While further improvements in the retrieval algorithm and bias-correction method are needed, GOSAT and GOSAT-2 retrievals are generally in good agreement.

Citation: Yoshida, Y., Y. Someya, H. Ohyama, I. Morino, T. Matsunaga, N. M. Deutscher, D. W. T. Griffith, F. Hase, L. T. Iraci, R. Kivi, J. Notholt, D. F. Pollard, Y. Té, V. A. Velazco, and D. Wunch, 2023: Quality evaluation of the column-averaged dry air mole fractions of carbon dioxide and methane observed by GOSAT and GOSAT-2. *SOLA*, **19**, 173−184, doi:10.2151/sola.2023-023.

1. Introduction

Atmospheric carbon dioxide (CO_2) and methane (CH_4) are well-known major anthropogenic greenhouse gases. Monitoring the concentrations and fluxes of these gases on global and regional scales is important, and satellite observations of the column-averaged dry-air mole fractions of these gases (XCO_2 and XCH_4, hereinafter called Xgas) in the atmosphere are expected to overcome these challenges (Rayner and O'Brien 2001; Chevallier et al. 2007, 2009; Takagi et al. 2011, 2021). The GOSAT Series is a series of Japanese Earth observation satellites to monitor the global distribution of CO_2 and CH_4 from space, and the GOSAT Series mission is promoted by the Ministry of the Environment Government of Japan, NIES (National Institute for Environmental Studies), and JAXA (Japan Aerospace Exploration Agency). GOSAT (Greenhouse gases Observing SATellite; launched on 23 January 2009) and GOSAT-2 (launched on 29 October 2018) are in operation, and to continue long-term monitoring of Xgas, GOSAT-GW (Global Observing SATellite for Greenhouse gases and Water cycle) is scheduled for launch in the Japanese fiscal year 2024. GOSAT Xgas is retrieved from SWIR (Short-Wavelength InfraRed) spectral data obtained by the TANSO-FTS (Thermal And Near Infrared Sensor for carbon Observation-Fourier Transform Spectrometer) onboard GOSAT using a so-called full-physics retrieval method developed by NIES (Yoshida et al. 2013). The retrieval algorithm for GOSAT-2 is developed based on that for GOSAT and optimized to the GOSAT-2 specifications. Table 1 summarizes the state vector elements

Corresponding author: Yukio Yoshida, National Institute for Environmental Studies, 16-2 Onogawa, Tsukuba, Ibaraki 305-8506, Japan. E-mail: yoshida.yukio@nies.go.jp.

Table 1. State vector elements and their a priori data of the full-physics retrieval method for (a) GOSAT and (b) GOSAT-2. Full spelling of the dataset and references are given outside the table.

(a) GOSAT

State vector elements	A priori data
CO_2 profile (15 layers)	NIES TM[1)]
CH_4 profile (15 layers)	NIES TM[1)]
H_2O profile (15 layers)	JMA GPV[2)]
aerosol profile (6 layers, 2 types)	SPRINTARS (free run)[3)]
surface pressure	JMA GPV[2)]
temperature shift	JMA GPV[2)]
surface albedo (for land case, zigzag approximation)	MOD43B3[4)]
surface wind speed (for ocean case)	JMA GPV[2)]
zero-level offset (for Band 1)	0.0
wavenumber dispersion correction factor	0.0

(b) GOSAT-2

State vector elements	A priori data
CO_2 profile (15 layers)	NICAM TM[5)]
CH_4 profile (15 layers)	NICAM TM[5)]
CO profile (15 layers)	MOZART-4[6)]
H_2O profile (15 layers)	JMA JRA-55[7)]
aerosol profile (15 layers, 2 types)	SPRINTARS (free run)[3)]
surface pressure	JMA JRA-55[7)]
temperature shift	JMA JRA-55[7)]
surface albedo (zigzag approximation)	averaged surface reflectance[8)]
chlorophyll fluorescence (SIF at reference wavenumber)	1.0×10^{-9} [W/cm^2/str/cm^{-1}]
chlorophyll fluorescence (slope for wavenumber)	0.0018 [cm]
zero-level offset	0.0 [W/cm^2/str/cm^{-1}]
wavenumber dispersion correction factor	0.0
Instrumental line shape function stretch factor	1.0

1) NIES atmospheric tracer Transport Model (Saeki et al. 2013)
2) Japan Meteorological Agency (JMA) Grid Point Value meteorological dataset (JMA 2007)
3) Spectral Radiation-Transport Model for Aerosol Species (Takemura et al. 2000)
4) Moderate Resolution Imaging Spectroradiometer (MODIS) land surface albedo product (Schaaf et al. 2002)
5) Nonhydrostatic Icosahedral Atmospheric Model (NICAM) Transport Model (Niwa et al. 2011)
6) Model for Ozone and Related Chemical Tracers version 4 (Emmons et al. 2010)
7) Japanese 55-year Reanalysis (Kobayashi et al. 2015)
8) see Section 4.7.5.7 of Yoshida and Oshio (2022)

to be retrieved and their a priori information (see Yoshida et al. 2017 and Yoshida and Oshio 2022 for more detail about the retrieval algorithm). Since satellite retrieval data can show some bias, it is important to validate it using independent data and to correct for such biases. Updates to the retrieval algorithm and/or the validation of the retrieval results for each satellite are independently conducted. To make long-term Xgas data from the GOSAT Series useful, it is also important to evaluate the degree to which the Xgas data is consistent across satellites. This paper presents a first attempt to evaluate the quality of GOSAT-2 Xgas and the degree of inter-satellite consistency of GOSAT and GOSAT-2 Xgas.

2. GOSAT and GOSAT-2

GOSAT is in a sun-synchronous orbit at 666-km altitude with a three-day revisit cycle. GOSAT is equipped with two instruments: TANSO-FTS and TANSO-CAI (Cloud and Aerosol Imager) (Kuze et al. 2009). The TANSO-FTS IFOV (instantaneous field of view) is 15.8 mrad, which corresponds to a nadir footprint diameter of about 10.5 km. The TANSO-FTS has a pointing mechanism that allows observation in off-nadir directions. Since August 2010, the TANSO-FTS has been operating in a 3-point cross-track scan mode to improve pointing stability (Crisp et al. 2012). In this mode, footprints are separated by ~280 km and each footprint is sampled three times. Due to the low reflectance of the ocean surface except for the sun-glint direction, the TANSO-FTS operates in sun-glint mode over ocean to track a sun-glint region with a pointing angle of ±20 degrees in the along-track direction. The TANSO-CAI is a nadir-viewing push-broom imager that provides cloud and aerosol information at 0.5 km spatial resolution within the IFOV of TANSO-FTS.

GOSAT-2 is in a sun-synchronous orbit at 613-km altitude with a six-day revisit cycle. GOSAT-2 is also equipped with two instruments: TANSO-FTS-2 (Suto et al. 2021) and TANSO-CAI-2. The TANSO-FTS-2 IFOV is also 15.8

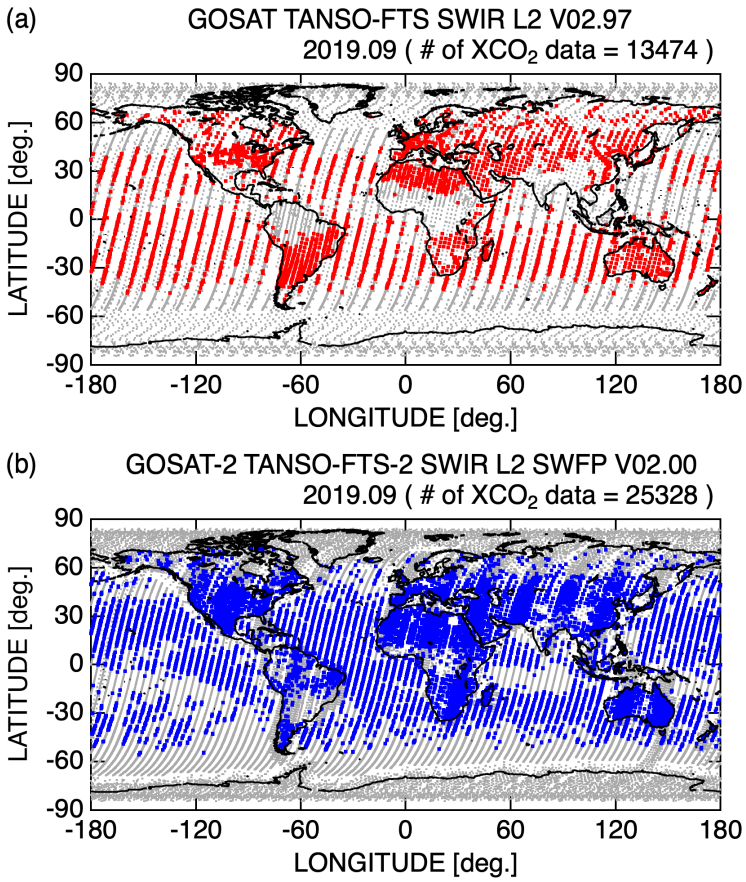

Fig. 1. Locations of observation points in September 2019 by (a) TANSO-FTS and (b) TANSO-FTS-2. Grey dots indicate observation points and red or blue dots indicate observation points for which the SWIR L2 XCO_2 data are available.

mrad, corresponding to a nadir footprint diameter of about 9.7 km. TANSO-FTS-2 has a new function named intelligent pointing, that shifts the instrument's line-of-sight to the cloud-free region when TANSO-FTS-2 detects clouds within the TANSO-FTS-2 IFOV by on-orbit operation, to increase cloud-free data. In addition, the latitudinal range of the sunglint mode is wider than that of TANSO-FTS because the maximum pointing angle in the along-track direction is ±40 degrees.

Figures 1a and 1b show examples of the TANSO-FTS and TANSO-FTS-2 observation points in September 2019, respectively. The TANSO-FTS-2 has a higher spatial density of observation points than TANSO-FTS due to an increase in the number of revolutions for a recurrence associated with the longer revisit cycle of GOSAT-2 and changing the nominal observation pattern. Furthermore, the above-mentioned improvements to TANSO-FTS-2, i.e., the intelligent pointing and the expanded pointing range, have approximately doubled the number of Xgas data and expanded spatial coverage.

3. Data

3.1 Bias-corrected Xgas data from GOSAT TANSO-FTS

The TANSO-FTS SWIR L2 (Level 2) V02.90 (April 2009 ~ May 2020) and V02.91 (June 2020 ~ present) contain Xgas from cloud-free observations retrieved from the TANSO-FTS L1B (Level 1B) V220.220 and V220.221, respectively. In June 2020, the ZPD (zero path difference) shifts in the TANSO-FTS (see section 3.1 of Kuze et al. 2016 for detail) increased such that the TANSO-FTS L1B V220.220 processing could no longer handle it. The V220.221 processing addresses this problem and does not differ in data quality from V220.220. In other words, SWIR L2 V02.90 and V02.91 also do not differ in data quality. The retrieved Xgas shows systematic biases that depend on simultaneously retrieved auxiliary parameters. Therefore, the bias correction is conducted by multiple regression analysis with explanatory variables described in Inoue et al. (2016) to create bias-corrected products V02.95 and V02.96 (NIES GOSAT project 2021a) from V02.90 and V02.91, respectively. In addition, a simple regression analysis is added to correct the annual growth rate of the bias-corrected XCO_2 over the ocean to create V02.97 and V02.98 (NIES GOSAT project 2021b). The correction formulae and its coefficients are different for land and ocean and are shown in section 3 of NIES GOSAT project (2021a, 2021b). The bias-corrected products V02.97 and V02.98 for XCO_2 and V02.95 and V02.96 for

XCH_4 are used in this study (hereinafter called GOSAT Xgas). The changes in XCO_2 over the land, XCH_4 over the land, and XCH_4 over the ocean due to this correction are mostly distributed between −4 ppm and 4 ppm, between −10 ppb and 15 ppb, and between −15 ppb and 20 ppb, respectively, regardless of time. On the other hand, the changes in XCO_2 over the ocean increases with time and are mostly distributed between −2 ppm and 4 ppm in April 2009 and between 0 ppm and 6 ppm in December 2020.

3.2 Bias-corrected Xgas data from GOSAT-2 TANSO-FTS-2

Recently, the TANSO-FTS-2 SWIR L2 Column-averaged Dry-air Mole Fraction Product was updated to V02.00 (Yoshida and Oshio 2022). This product contains the bias-uncorrected Xgas from cloud-free observations. To reduce systematic biases, the following bias corrections are applied in this study (hereinafter bias-corrected Xgas are called GOSAT-2 Xgas).

$$XCO_2^{Bias-Corrected} = XCO_2 + A_0 + A_1 \cdot \Delta P_S + A_2 \cdot AOT + A_3 \cdot fILS_{SB2} \quad (1)$$

$$XCH_4^{Bias-Corrected} = XCH_4 + B_0 + B_1 \cdot \Delta P_S + B_2 \cdot AOT + B_3 \cdot fILS_{SB5} \quad (2)$$

where ΔP_S is the difference between the retrieved and a priori surface pressure (hPa), AOT is the retrieved aerosol optical thickness, and $fILS$ is the retrieved ILS (instrumental line shape) stretch factor for sub-band indicated by the subscript. The coefficients A_0, A_1, A_2, A_3, B_0, B_1, B_2, and B_3 are −0.89863, 0.236607, -1.64121×10^2, −1.53897, 0.529805, 1.13007×10^{-3}, −0.320115, and −0.525923, respectively, and the unit for Xgas is ppm. There is no distinction between land and ocean in these coefficients. The changes in XCO_2 due to this correction are mostly distributed between −5 ppm and 4 ppm for land and between −10 ppm and −1 ppm for ocean, respectively, and those in XCH_4 are mostly distributed between −5 ppb and 45 ppb for land and between −25 ppb and 15 ppb for ocean, respectively.

3.3 TCCON data

The TCCON (Total Carbon Column Observing Network) is a network of ground-based Fourier Transform Spectrometers whose Xgas data are widely used to validate satellite Xgas (Wunch et al. 2011). Although version GGG2020 of the TCCON data is recently released, version GGG2014 (Griffith et al. 2014a, 2014b; Hase et al. 2015; Iraci et al. 2016; Kawakami et al. 2014; Kivi et al. 2020; Morino et al. 2018a, 2018b; Notholt et al. 2019; Petri et al. 2020; Pollard et al. 2019; Sherlock et al. 2014; Té et al. 2014; Warneke et al. 2019; Wennberg et al. 2015, 2016a, 2016b, 2017; Wunch et al. 2018) is used in this paper because it was used as the ground-truth in the bias correction of the TANSO-FTS and TANSO-FTS-2 SWIR L2 products described above. The uncertainties of Xgas from TCCON (2σ) are 0.8 ppm and 7 ppb for XCO_2 and XCH_4, respectively (Wunch et al. 2010).

4. Results and discussions

First, GOSAT and GOSAT-2 Xgas data are compared with TCCON data. For comparison, satellite data are selected within a ±0.2° latitude-longitude box centered on each TCCON site with a difference of less than 200 m between the mean altitude within the FTS IFOV and the TCCON site altitude. The TCCON data is the mean values measured at each TCCON site within ±30 min of satellite observation time. The strict condition of ±0.2° is used to minimize the impact of spatial variation in Xgas on the evaluation results. Due to the strict conditions of ±0.2°, comparisons are limited to land data. The site bias and the single measurement precision of satellite data defined as average and standard deviation of differences to TCCON data, respectively, are calculated for each TCCON site. Using these values for TCCON sites with more than 20 matched data, averaged site bias, site-to-site bias defined as the standard deviation of the site bias, and averaged single measurement precision are calculated. The results for TCCON sites with at least 20 matched data for one of the two satellites are shown in Table 2 and the time series of Xgas from the satellites and TCCON sites at TCCON sites with at least 20 matched data for each of the two satellites during the common observation period are shown in Fig. 2. Both GOSAT and GOSAT-2 data are shown to capture seasonal variation in Xgas. The averaged single measurement precision for XCO_2 and XCH_4 are less than 1.9 ppm and 10 ppb, respectively, with the site-to-site biases of less than 0.9 ppm and 5 ppb, respectively. Although common TCCON sites are limited due to different observation patterns, GOSAT-2 seems to be as accurate and precise as GOSAT.

Next, a comparison of the individual Xgas data for GOSAT and GOSAT-2 is made. For each GOSAT-2 data, the closest same-day GOSAT data within a ±0.2° latitude-longitude box with an IFOV-mean altitude difference of 200 m or less are selected. Most of the observed time differences for the matched data are within 15 min. Although the matched data are only available for specific locations due to the satellite orbits, the ocean data are also comparable, unlike the TCCON comparison. The matched data are in good agreement overall, with a slight bias in XCH_4 over the ocean (Fig. 3). The standard deviations of XCO_2 and XCH_4 differences for all data are 2.18 ppm and 12.1 ppb, respectively, which are slightly smaller than the root sum square of the averaged single measurement precision of GOSAT and GOSAT-2.

Table 2. Summary of the comparison between GOSAT/GOSAT-2 products and TCCON measurements for (a) XCO_2 and (b) XCH_4. N, A, and σ indicate the number of matched data, the average of their differences (site bias), and the standard deviation of their differences (single measurement precision), respectively. The averaged site bias, site-to-site bias (standard deviation of A), and averaged single measurement precision are also shown at the bottom of the table for only sites having at least 20 matched data with the satellite ones. TCCON sites with less than 20 matched data for both GOSAT and GOSAT-2 are not shown in the table. For GOSAT, results for the same period as GOSAT-2 are also shown for reference.

(a) XCO_2

site	latitude [°N]	longitude [°E]	GOSAT (2009/04 ~ 2020/12)			GOSAT-2 (2019/03 ~ 2020/12)			GOSAT (2019/03 ~ 2020/12)		
			N	A [ppm]	σ [ppm]	N	A [ppm]	σ [ppm]	N	A [ppm]	σ [ppm]
sodankyla01	67.37	26.63	42	−0.31	1.83	12	−0.65	1.60	16	−0.87	2.28
easttroutlake01	54.36	−104.99	0	–	–	35	−1.44	2.97	0	–	–
bremen01	53.10	8.85	26	0.77	1.97	12	−0.61	1.06	2	−0.19	1.88
karlsruhe01	49.10	8.44	0	–	–	83	0.71	2.42	0	–	–
paris01	48.85	2.36	13	−0.41	1.65	49	0.94	1.92	5	0.64	0.66
orleans01	47.97	2.11	49	0.82	1.62	56	0.60	1.54	16	0.76	1.60
parkfalls01	45.95	−90.27	486	−0.53	1.90	72	−0.95	2.91	37	−0.87	2.82
lamont01	36.60	−97.49	275	−0.24	1.42	263	0.53	1.39	42	0.00	1.47
tsukuba02	36.05	140.12	240	0.97	1.69	31	0.33	1.53	11	0.44	0.94
nicosia01	35.14	33.38	0	–	–	89	0.45	1.38	0	–	–
edwards01	34.96	−117.88	628	−0.22	1.27	301	0.51	1.44	169	−0.30	1.46
jpl02	34.20	−118.18	106	0.98	1.99	0	–	–	0	–	–
pasadena01	34.14	−118.13	1128	−0.36	1.54	478	−0.68	1.24	266	−1.00	1.38
saga01	33.24	130.29	108	1.00	1.55	93	0.47	1.44	35	1.42	1.47
burgos01	18.53	120.65	20	2.43	1.76	8	0.22	1.89	11	1.19	1.26
darwin01	−12.43	130.89	20	2.03	2.34	15	−0.80	2.03	0	–	–
wollongong01	−34.41	150.88	9	−1.57	1.20	20	−0.51	1.82	0	–	–
lauder02	−45.04	169.68	163	−0.05	1.62	0	–	–	0	–	–
lauder03	−45.04	169.68	31	0.58	1.34	129	−0.14	1.58	31	0.58	1.34
averaged site bias			14	0.56		13	0.06		6	(−0.02)	
site-to-site bias			14	0.88		13	0.71		6	(0.83)	
averaged single measurement precision			14	1.70		13	1.81		6	(1.66)	

(b) XCH_4

site	latitude [°N]	longitude [°E]	GOSAT (2009/04 ~ 2020/12)			GOSAT-2 (2019/03 ~ 2020/12)			GOSAT (2019/03 ~ 2020/12)		
			N	A [ppb]	σ [ppb]	N	A [ppb]	σ [ppb]	N	A [ppb]	σ [ppb]
sodankyla01	67.37	26.63	43	3.8	13.0	12	1.9	8.1	17	0.9	13.9
easttroutlake01	54.36	−104.99	0	–	–	36	−0.9	12.3	0	–	–
bremen01	53.10	8.85	26	6.5	12.1	12	−2.0	4.2	2	−4.7	12.5
karlsruhe01	49.10	8.44	0	–	–	83	3.2	9.1	0	–	–
paris01	48.85	2.36	13	−0.5	5.5	49	−0.2	8.7	5	4.2	3.2
orleans01	47.97	2.11	49	2.8	8.0	56	2.3	6.1	16	−0.4	7.2
parkfalls01	45.95	−90.27	486	2.4	10.0	72	−0.5	12.4	37	−2.4	13.8
lamont01	36.60	−97.49	275	0.7	9.3	263	1.3	8.6	42	1.2	8.7
tsukuba02	36.05	140.12	240	4.1	9.6	31	0.5	10.6	11	0.5	4.
nicosia01	35.14	33.38	0	–	–	89	2.0	8.1	0	–	–
edwards01	34.96	−117.88	628	0.8	7.8	301	−0.3	8.5	169	0.2	8.4
jpl02	34.20	−118.18	106	1.8	9.5	0	–	–	0	–	–
pasadena01	34.14	−118.13	1128	−1.0	9.0	478	−2.8	6.7	266	−1.8	8.3
saga01	33.24	130.29	108	8.9	9.0	93	5.1	10.0	35	12.6	7.8
burgos01	18.53	120.65	20	10.9	6.0	8	−2.4	7.0	11	8.8	4.3
darwin01	−12.43	130.89	20	9.8	8.3	15	−5.7	4.8	0	–	–
wollongong01	−34.41	150.88	9	−2.4	16.1	20	−0.9	7.5	0	–	–
lauder02	−45.04	169.68	163	−1.9	9.2	0	–	–	0	–	–
lauder03	−45.04	169.68	31	−1.9	7.9	177	1.9	7.5	31	−1.9	7.9
averaged site bias			14	3.4		13	0.8		6	(1.3)	
site-to-site bias			14	4.1		13	2.0		6	(5.2)	
averaged single measurement precision			14	9.2		13	8.9		6	(9.2)	

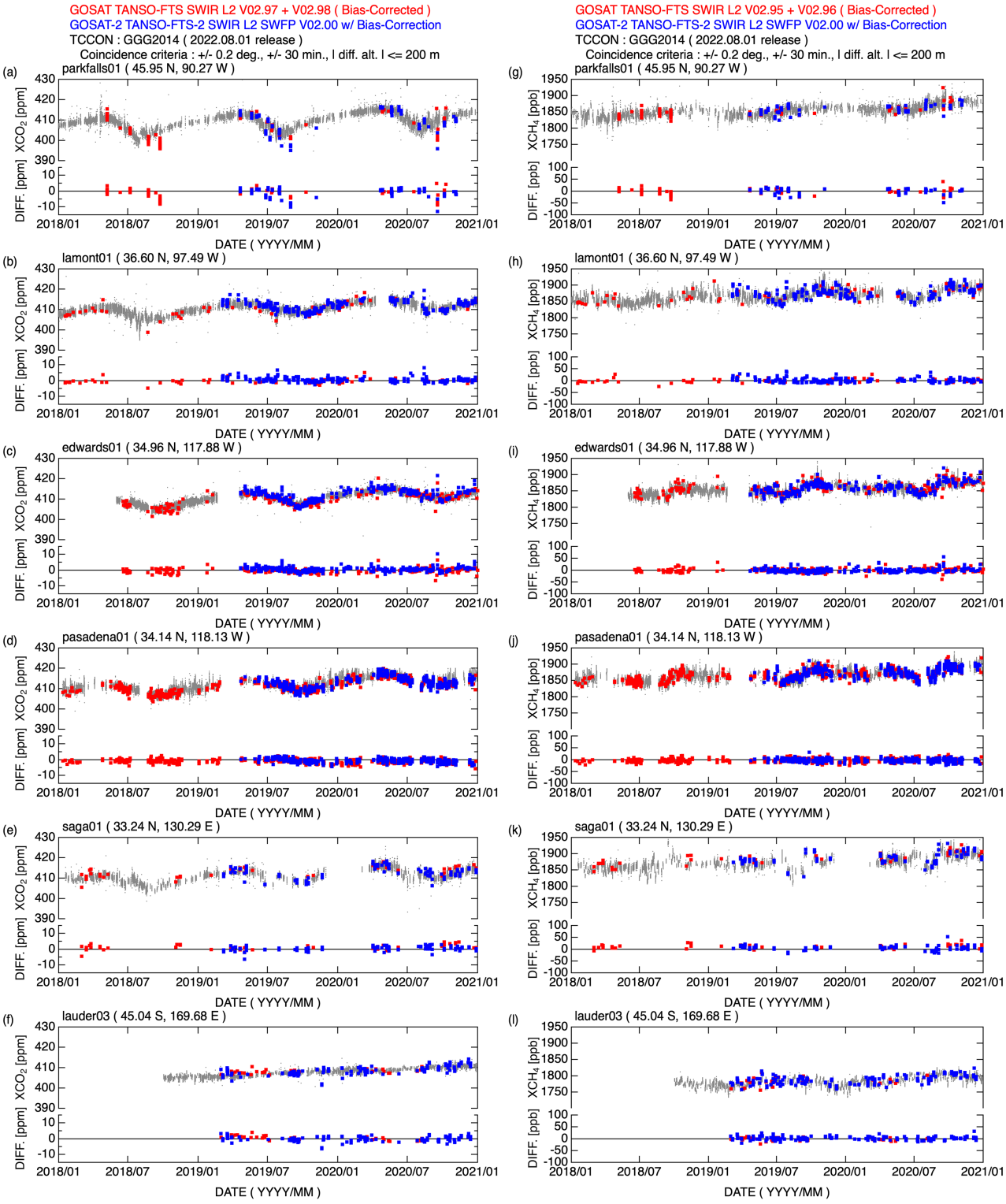

Fig. 2. Time series of the GOSAT (red), GOSAT-2 (blue), and TCCON (grey) and their differences from TCCON. Only TCCON sites with at least 20 matched data for each of GOSAT and GOSAT-2 during the common observation period are shown. (a ~ f) XCO_2 and (g ~ l) XCH_4 for each TCCON site.

The ocean bias in XCH_4 might be due to the fact that the state vector elements and the coefficients of the bias correction are different between land and ocean for GOSAT, while they are identical for GOSAT-2, but the details are beyond the scope of this paper.

To examine the degree of the regional dependence, Figs. 4 and 5 show the difference between the monthly averages of Xgas within 10° × 10° grid box for GOSAT and GOSAT-2 (see Supplement 1 for the monthly averaged Xgas for each satellite). Note that this difference includes differences in observation points and times between satellites. The

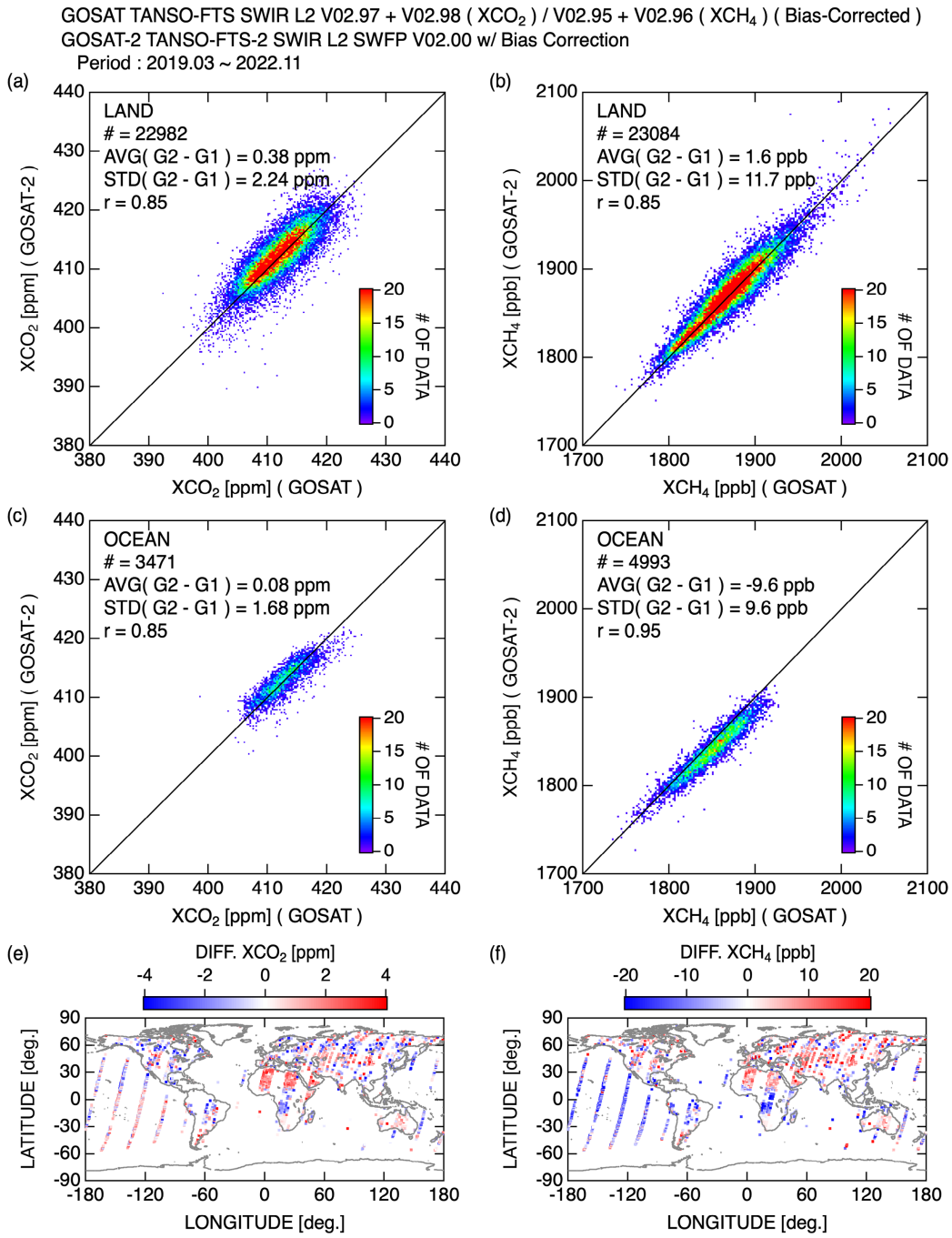

Fig. 3. Two-dimensional histograms of individual matched data for GOSAT and GOSAT-2: (a) land XCO_2, (b) land XCH_4, (c) ocean XCO_2, and (d) ocean XCH_4. The locations of the matched data colored by Xgas difference (GOSAT-2 minus GOSAT): (e) XCO_2 and (f) XCH_4. G1 for GOSAT and G2 for GOSAT-2.

differences in averaged Xgas show not only regional dependence but also time dependence, mainly seasonal variation (Figs. S7, S8). The causes of these dependence are still under investigation, but it appears to be largely due to insufficient representation of the optical path modification due to atmospheric scattering. For example, the positive difference in North Africa may be due to an overestimation of Xgas by GOSAT-2 because the simultaneously retrieved aerosol optical thickness was smaller than that by GOSAT. The standard deviations of the averaged Xgas difference using grids with more than 10 measurements for both satellites are 1.77 ppm and 11.7 ppb for XCO_2 and XCH_4, respectively. These values are larger than the site-to-site biases evaluated in the TCCON comparison, suggesting that the number of TCCON sites used for evaluating the site-to-site biases would be insufficient to cover the global diversity of observation points and to obtain more appropriate regional dependence of the bias. Therefore, it is important to obtain additional ground-based validation data that covers the different range of the satellite measurands and geographical coverage, such as higher albedo (> 0.5) areas or ocean. Since the regional patterns of monthly-regional averaged Xgas differences are

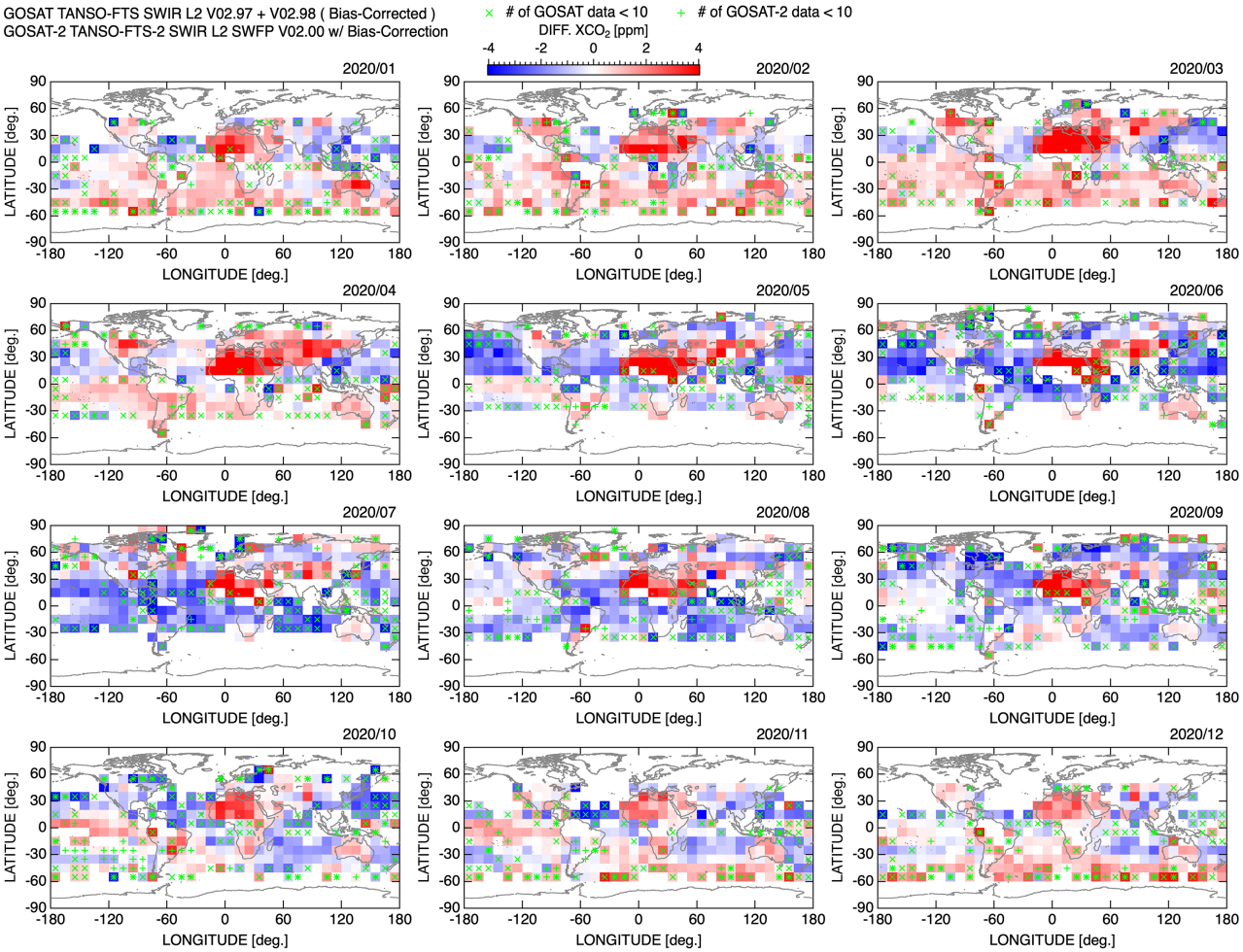

Fig. 4. The difference between the monthly averages of XCO_2 within 10° × 10° grid box for GOSAT and GOSAT-2 in 2020 (GOSAT-2 minus GOSAT). Cross and plus marks indicate that the number of Xgas data used to calculate the monthly average is less than 10 for GOSAT and GOSAT-2, respectively.

similar to the patterns of individual Xgas differences, it can be assumed that as the consistency of individual Xgas data improves, the consistency of the monthly-regional averaged Xgas will also improve.

5. Conclusion

The quality and degree of inter-satellite consistency of GOSAT and GOSAT-2 Xgas are evaluated. A comparison of each satellite data with TCCON data showed that the averaged single measurement precision for XCO_2 and XCH_4 are less than 1.9 ppm and 10 ppb, respectively, with the site-to-site biases of less than 0.9 ppm and 5 ppb, respectively, although the TCCON sites used for evaluation are different due to differences in observation patterns of satellites. The inter-satellite comparison shows that GOSAT and GOSAT-2 retrievals are generally in good agreement with the standard deviations of 2.18 ppm and 12.1 ppb for individual XCO_2 and XCH_4 differences, respectively, and those of 1.77 ppm and 11.7 ppb for monthly regional averaged XCO_2 and XCH_4 differences, respectively. The difference between the TCCON comparison results and the inter-satellite comparison results indicates the need for additional validation sites and further bias reduction in satellite Xgas.

Acknowledgements

The GOSAT data is available from the GOSAT Data Archive Service (https://data2.gosat.nies.go.jp/, last access: March 2023). The GOSAT-2 data is available from the GOSAT-2 Product Archive (https://prdct.gosat-2.nies.go.jp/, last access: March 2023). The TCCON data were obtained from the TCCON Data Archive hosted by CaltechDATA at https://tccondata.org/. The Paris TCCON site has received funding from Sorbonne Université, the French research center CNRS, the French space agency CNES, and Région Île-de-France.

Edited by: H. Irie

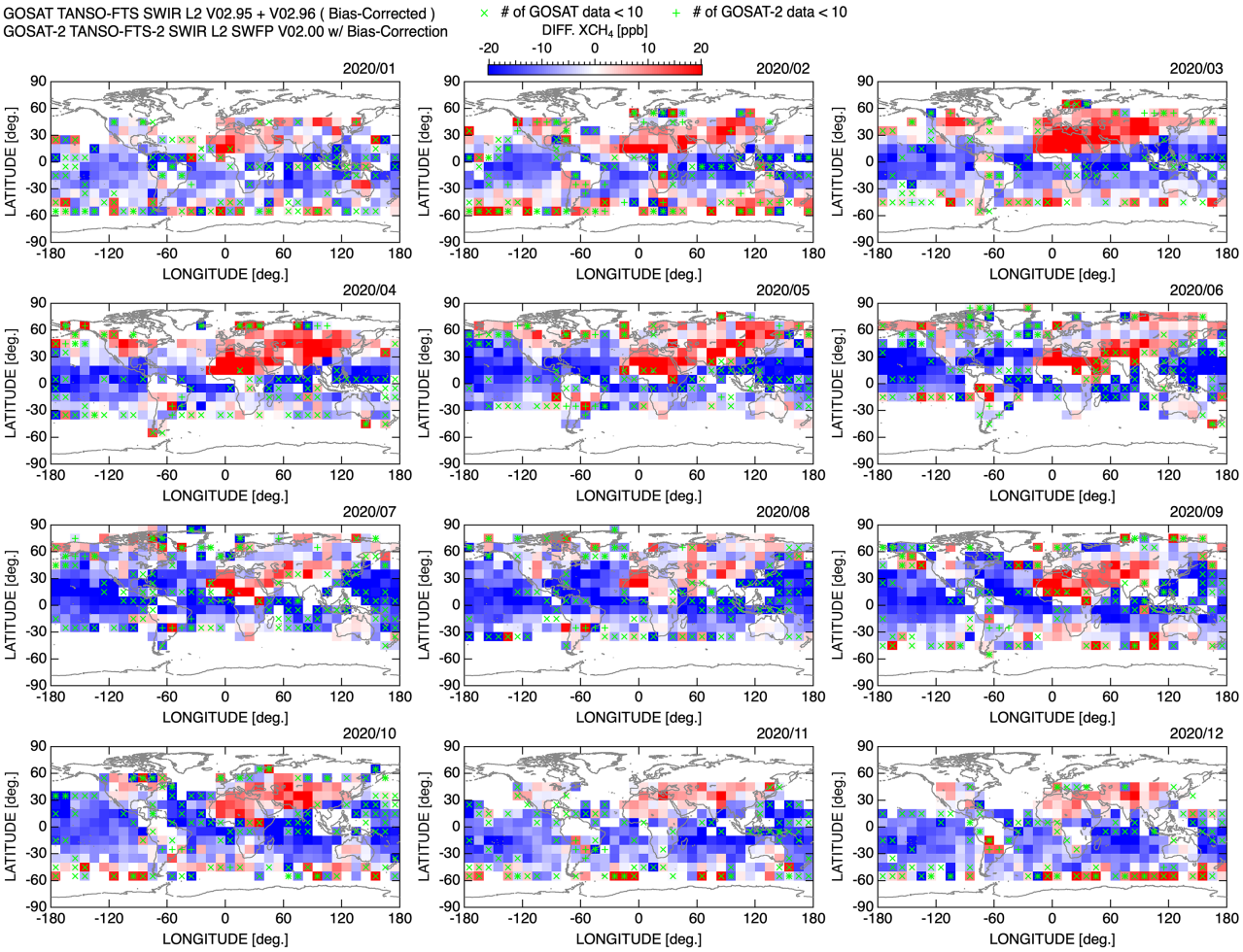

Fig. 5. Same as Fig. 4 but for XCH_4.

Supplements

Supplement 1: Monthly averages of Xgas within 10° × 10° grid box for GOSAT and GOSAT-2

References

Chevallier, F., F.-M. Bréon, and P. J. Rayner, 2007: Contribution of the Orbiting Carbon Observatory to the estimation of CO_2 sources and sinks: Theoretical study in a variational data assimilation framework. *J. Geophys. Res.*, **112**, D09307, doi:10.1029/2006JD007375.

Chevallier, F., S. Maksyutov, P. Bousquet, F.-M. Bréon, R. Saito, Y. Yoshida, and T. Yokota, 2009: On the accuracy of the CO_2 surface fluxes to be estimated from the GOSAT observations. *Geophys. Res. Lett.*, **36**, L19807, doi: 10.1029/2009GL040108.

Crisp, D., B. M. Fisher, C. O'Dell, C. Frankenberg, R. Basilio, H. Bösch, L. R. Brown, R. Castano, B. Connor, N. M. Deutscher, A. Eldering, D. Griffith, M. Gunson, A. Kuze, L. Mandrake, J. McDuffie, J. Messerschmidt, C. E. Miller, I. Morino, V. Natraj, J. Notholt, D. M. O'Brien, F. Oyafuso, I. Polonsky, J. Robinson, R. Salawitch, V. Sherlock, M. Smyth, H. Suto, T. E. Taylor, D. R. Thompson, P. O. Wennberg, D. Wunch, and Y. L. Yung, 2012: The ACOS CO_2 retrieval algorithm - Part II: Global XCO_2 data characterization. *Atmos. Meas. Tech.*, **5**, 687–707, doi:10.5194/amt-5-687-2012.

Emmons, L. K., S. Walters, P. G. Hess, J.-F. Lamarque, G. G. Pfister, D. Fillmore, C. Granier, A. Guenther, D. Kinnison, T. Laepple, J. Orlando, X. Tie, G. Tyndall, C. Wiedinmyer, S. L. Baughcum, and S. Kloster, 2010: Description and evaluation of the Model for Ozone and Related chemical Tracers, version 4 (MOZART-4). *Geosci. Model Dev.*, **3**, 43–67, doi:10.5194/gmd-3-43-2010.

Griffith, D. W. T., N. M. Deutscher, V. A. Velazco, P. O. Wennberg, Y. Yavin, G. Keppel-Aleks, R. A. Washenfelder, G. C. Toon, J.-F. Blavier, C. Paton-Walsh, N. B. Jones, G. C. Kettlewell, B. J. Connor, R. C. Macatangay, C. Roehl, M. Ryczek, J. Glowacki, T. Culgan, and G. W. Bryant, 2014a: TCCON data from Darwin, Australia, Release GGG2014R0. TCCON data archive, hosted by CaltechDATA, California Institute of Technology, Pasadena, CA,

U.S.A., https://doi.org/10.14291/tccon.ggg2014.darwin01.R0/1149290.

Griffith, D. W. T., V. A. Velazco, N. M. Deutscher, C. Paton-Walsh, N. B. Jones, S. R. Wilson, R. C. Macatangay, G. C. Kettlewell, R. R. Buchholz, and M. O. Riggenbach, 2014b: TCCON data from Wollongong, Australia, Release GGG2014R0. TCCON data archive, hosted by CaltechDATA, California Institute of Technology, Pasadena, CA, U.S.A., https://doi.org/10.14291/tccon.ggg2014.wollongong01.R0/1149291.

Hase, F., T. Blumenstock, S. Dohe, J. Groß, and M. Kiel, 2015: TCCON data from Karlsruhe, Germany, Release GGG2014R1. TCCON data archive, hosted by CaltechDATA, California Institute of Technology, Pasadena, CA, U.S.A., https://doi.org/10.14291/tccon.ggg2014.karlsruhe01.R1/1182416.

Inoue, M., I. Morino, O. Uchino, T. Nakatsuru, Y. Yoshida, T. Yokota, D. Wunch, P. O. Wennberg, C. M. Roehl, D. W. T. Griffith, V. A. Velazco, N. M. Deutscher, T. Warneke, J. Notholt, J. Robinson, V. Sherlock, F. Hase, T. Blumenstock, M. Rettinger, R. Sussmann, E. Kyrö, R. Kivi, K. Shiomi, S. Kawakami, M. De Mazière, S. G. Arnold, D. G. Feist, E. A. Barrow, J. Barney, M. Dubey, M. Schneider, L. T. Iraci, J. R. Podolske, P. W. Hillyard, T. Machida, Y. Sawa, K. Tsuboi, H. Matsueda, C. Sweeney, P. P. Tans, A. E. Andrews, S. C. Biraud, Y. Fukuyama, J. V. Pittman, E. A. Kort, and T. Tanaka, 2016: Bias corrections of GOSAT SWIR XCO_2 and XCH_4 with TCCON data and their evaluation using aircraft measurement data. *Atmos. Meas. Tech.*, **9**, 3491–3512, doi:10.5194/amt-9-3491-2016.

Iraci, L. T., J. R. Podolske, P. W. Hillyard, C. Roehl, P. O. Wennberg, J.-F. Blavier, J. Landeros, N. Allen, D. Wunch, J. Zavaleta, E. Quigley, G. B. Osterman, R. Albertson, K. Dunwoody, and H. Boyden, 2016: TCCON data from Armstrong Flight Research Center, Edwards, CA, USA, Release GGG2014R1. TCCON data archive, hosted by CaltechDATA, California Institute of Technology, Pasadena, CA, U.S.A., https://doi.org/10.14291/tccon.ggg2014.edwards01.R1/1255068.

JMA, 2007: *Outline of the Operational Numerical Weather Prediction at the Japan Meteorological Agency*. (Available online at: https://www.jma.go.jp/jma/jma-eng/jma-center/nwp/outline2007-nwp/index.htm, accessed 18 May 2023)

Kawakami, S., H. Ohyama, K. Arai, H. Okumura, C. Taura, T. Fukamachi, and M. Sakashita, 2014: TCCON data from Saga, Japan, Release GGG2014R0. TCCON data archive, hosted by CaltechDATA, California Institute of Technology, Pasadena, CA, U.S.A., https://doi.org/10.14291/tccon.ggg2014.saga01.R0/1149283.

Kivi, R., P. Heikkinen, and E. Kyrö, 2020: TCCON data from Sodankylä, Finland, Release GGG2014R1. TCCON data archive, hosted by CaltechDATA, California Institute of Technology, Pasadena, CA, U.S.A., https://doi.org/10.14291/tccon.ggg2014.sodankyla01.R1.

Kobayashi, S., Y. Ota, Y. Harada, A. Ebita, M. Moriya, H. Onoda, K. Onogi, H. Kamahori, C. Kobayashi, H. Endo, K. Miyaoka, and K. Takahashi, 2015: The JRA-55 reanalysis: General specifications and basic characteristics. *J. Meteor. Soc. Japan*, **93**, 5–48, doi:10.2151/jmsj.2015-001.

Kuze, A., H. Suto, M. Nakajima, and T. Hamazaki, 2009: Thermal and near infrared sensor for carbon observation Fourier-transform spectrometer on the Greenhouse Gases Observing Satellite for greenhouse gases monitoring. *Appl., Opt.*, **48**, 6716–6733, doi:10.1364/AO.48.006716.

Kuze, A., H. Suto, K. Shiomi, S. Kawakami, M. Tanaka, Y. Ueda, A. Deguchi, J. Yoshida, Y. Yamamoto, F. Kataoka, T. E. Taylor, and H. L. Buijs, 2016: Update on GOSAT TANSO-FTS performance, operations, and data products after more than 6 years in space. *Atmos. Meas. Tech.*, **9**, 2445–2461, doi:10.5194/amt-9-2445-2016.

Morino, I., T. Matsuzaki, and M. Horikawa, 2018a: TCCON data from Tsukuba, Ibaraki, Japan, 125HR, Release GGG2014R2. TCCON data archive, hosted by CaltechDATA, California Institute of Technology, Pasadena, CA, U.S.A., https://doi.org/10.14291/tccon.ggg2014.tsukuba02.R2.

Morino, I., V. A. Velazco, A. Hori, O. Uchino, and D. W. T. Griffith, 2018b: TCCON data from Burgos, Philippines, Release GGG2014R0. TCCON data archive, hosted by CaltechDATA, California Institute of Technology, Pasadena, CA, U.S.A., https://doi.org/10.14291/tccon.ggg2014.burgos01.R0/1368175.

NIES GOSAT Project, 2021a: Release Note of Bias-Corrected FTS SWIR Level 2 CO_2, CH_4 Products (V02.95/V02.96) for General Users. (Available online at: https://data2.gosat.nies.go.jp/doc/documents/ReleaseNote_FTSSWIRL2_BiasCorr_V02.95-V02.96_en.pdf, accessed 17 May 2023)

NIES GOSAT Project, 2021b: Release Note of Bias-Corrected FTS SWIR Level 2 CO_2 Product (V02.97/V02.98) for General Users. (Available online at: https://data2.gosat.nies.go.jp/doc/documents/ReleaseNote_FTSSWIRL2_BiasCorrCO2_V02.97-V02.98_en.pdf, accessed 9 March 2023)

Niwa, Y., H. Tomita, M. Satoh, and R. Imasu, 2011: A three-dimensional icosahedral grid advection scheme preserving monotonicity and consistency with continuity for atmospheric tracer transport. *J. Meteor. Soc. Japan*, **89**, 255–268, doi:10.2151/jmsj.2011-306.

Notholt, J., C. Petri, T. Warneke, N. M. Deutscher, M. Palm, M. Buschmann, C. Weinzierl, R. C. Macatangay, and P. Grupe, 2019: TCCON data from Bremen, Germany, Release GGG2014R1. TCCON data archive, hosted by CaltechDATA, California Institute of Technology, Pasadena, CA, U.S.A., https://doi.org/10.14291/tccon.ggg2014.bremen01.R1.

Petri, C., M. Vrekoussis, C. Rousogenous, T. Warneke, J. Sciare, and J. Notholt, 2020: TCCON data from Nicosia, Cyprus, Release GGG2014R0. TCCON data archive, hosted by CaltechDATA, California Institute of Technology, Pasadena, CA, U.S.A., https://doi.org/10.14291/tccon.ggg2014.nicosia01.R0.

Pollard, D. F., J. Robinson, and H. Shiona, 2019: TCCON data from Lauder, New Zealand, 125HR, Release GGG2014R0. TCCON data archive, hosted by CaltechDATA, California Institute of Technology, Pasadena, CA, U.S.A., https://doi.org/10.14291/tccon.ggg2014.lauder03.R0.

Rayner, P. J., and D. M. O'Brien, 2001: The utility of remotely sensed CO_2 concentration data in surface source inversions. *Geophys. Res. Lett.*, **28**, 175–178, doi:10.1029/2000GL011912.

Saeki, T., R. Saito, D. Belikov, and S. Maksyutov, 2013: Global high-resolution simulations of CO_2 and CH_4 using a NIES transport model to produce a priori concentrations for use in satellite data retrievals. *Geosci. Model Dev.*, **6**, 81–100, doi:10.5194/gmd-6-81-2013.

Schaaf, C. B., F. Gao, A. H. Strahler, W. Lucht, X. Li, T. Tsang, N. C. Strugnell, X. Zhang, Y. Jin, J.-P. Muller, P. Lewis, M. Barnsley, P. Hobson, M. Disney, G. Roberts, M. Dunderdale, C. Doll, R. P. d'Entremont, B. Hu, S. Liang, J. L. Privette, and D. Roy, 2002: First operational BRDF, albedo nadir reflectance products from MODIS. *Remote Sens. Environ.*, **83**, 135–148.

Sherlock, V., B. Connor, J. Robinson, H. Shiona, D. Smale, and D. F. Pollard, 2014: TCCON data from Lauder, New Zealand, 125HR, Release GGG2014R0. TCCON data archive, hosted by CaltechDATA, California Institute of Technology, Pasadena, CA, U.S.A., https://doi.org/10.14291/tccon.ggg2014.lauder02.R0/1149298.

Suto, H., F. Kataoka, N. Kikuchi, R. O. Knuteson, A. Butz, M. Haun, H. Buijs, K. Shiomi, H. Imai, and A. Kuze, 2021: Thermal and near-infrared sensor for carbon observation Fourier transform spectrometer-2 (TANSO-FTS-2) on the Greenhouse gases Observing SATellite-2 (GOSAT-2) during its first year in orbit. *Atmos. Meas. Tech.*, **14**, 2013–2039, doi:10.5194/amt-14-2013-2021.

Takagi, H., T. Saeki, T. Oda, M. Saito, V. Valsala, D. Belikov, R. Saito, Y. Yoshida, I. Morino, O. Uchino, R. J. Andres, T. Yokota, and S. Maksyutov, 2011: On the benefit of GOSAT observations to the estimation of regional CO_2 fluxes. *SOLA*, **7**, 161–164, doi:10.2151/sola.2011-041.

Takagi, H., A. Ito, H.-S. Kim, S. Maksyutov, M. Saito, and T. Matsunaga, 2021: Meteorological control of subtropical South American methane emissions estimated from GOSAT observations. *SOLA*, **17**, 213–219, doi:10.2151/sola.2021-037.

Takemura, T., H. Okamoto, Y. Maruyama, A. Numaguti, A. Higurashi, and T. Nakajima, 2000: Global three-dimensional simulation of aerosol optical thickness distribution of various origins. *J. Geophys. Res.*, **105**, 17853–17873.

Té, Y., P. Jeseck, and C. Janssen, 2014: TCCON data from Paris, France, Release GGG2014R0. TCCON data archive, hosted by CaltechDATA, California Institute of Technology, Pasadena, CA, U.S.A., https://doi.org/10.14291/tccon.ggg2014.paris01.R0/1149279.

Warneke, T., J. Messerschmidt, J. Notholt, C. Weinzierl, N. M. Deutscher, C. Petri, and P. Grupe, 2019. TCCON data from Orleans, France, Release GGG2014R1. TCCON data archive, hosted by CaltechDATA, California Institute of Technology, Pasadena, CA, U.S.A., https://doi.org/10.14291/tccon.ggg2014.orleans01.R1.

Wennberg, P. O., D. Wunch, C. M. Roehl, J.-F. Blavier, G. C. Toon, and N. T. Allen, 2015: TCCON data from California Institute of Technology, Pasadena, California, USA, Release GGG2014R1. TCCON data archive, hosted by CaltechDATA, California Institute of Technology, Pasadena, CA, U.S.A., https://doi.org/10.14291/tccon.ggg2014.pasadena01.R1/1182415.

Wennberg, P. O., D. Wunch, C. M. Roehl, J.-F. Blavier, G. C. Toon, and N. T. Allen, 2016a. TCCON data from Lamont, Oklahoma, USA, Release GGG2014R1. TCCON data archive, hosted by CaltechDATA, California Institute of Technology, Pasadena, CA, U.S.A., https://doi.org/10.14291/tccon.ggg2014.lamont01.R1/1255070.

Wennberg, P. O., C. M. Roehl, J.-F. Blavier, D. Wunch, and N. T. Allen, 2016b: TCCON data from Jet Propulsion Laboratory, Pasadena, California, USA, Release GGG2014R1. TCCON data archive, hosted by CaltechDATA, California Institute of Technology, Pasadena, CA, U.S.A., https://doi.org/10.14291/tccon.ggg2014.jpl02.R1/1330096.

Wennberg, P. O., C. M. Roehl, D. Wunch, G. C. Toon, J.-F. Blavier, R. Washenfelder, G. Keppel-Aleks, N. T. Allen, and J. Ayers, 2017: TCCON data from Park Falls, Wisconsin, USA, Release GGG2014R1. TCCON data archive, hosted by CaltechDATA, California Institute of Technology, Pasadena, CA, U.S.A., https://doi.org/10.14291/tccon.ggg2014.parkfalls01.R1.

Wunch, D., G. C. Toon, P. O. Wennberg, S. C. Wofsy, B. B. Stephens, M. L. Fischer, O. Uchino, J. B. Abshire, P. Bernath, S. C. Biraud, J.-F. L. Blavier, C. Boone, K. P. Bowman, E. V. Browell, T. Campos, B. J. Connor, B. C. Daube, N. M. Deutscher, M. Diao, J. W. Elkins, C. Gerbig, E. Gottlieb, D. W. T. Griffith, D. F. Hurst, R. Jiménez, G. Keppel-Aleks, E. A. Kort, R. Macatangay, T. Machida, H. Matsueda, F. Moore, I. Morino, S. Park, J. Robinson, C. M. Roehl, Y. Sawa, V. Sherlock. C. Sweeney, T. Tanaka, and M. A. Zondlo, 2010: Calibration of the total carbon column observing network using aircraft profile data. *Atmos. Meas. Tech.*, **3**, 1351–1362, doi:10.5194/amt-3-

1351-2010.

Wunch, D., G. C. Toon, J.-F. L. Blavier, R. A. Washenfelder, J. Notholt, B. J. Connor, D. W. T. Griffith, V. Sherlock, and P. O. Wennberg, 2011: The total carbon column observing network. *Phil. Trans. R. Soc. A*, **369**, 2087–2112, doi:10.1098/rsta.2010.0240.

Wunch, D., J. Mendonca, O. Colebatch, N. T. Allen, J.-F. Blavier, S. Roche, J. Hedelius, G. Neufeld, S. Springett, D. Worthy, R. Kessler, and K. Strong, 2018: TCCON data from East Trout Lake, Canada, Release GGG2014R1. TCCON data archive, hosted by CaltechDATA, California Institute of Technology, Pasadena, CA, U.S.A., https://doi.org/10.14291/tccon.ggg2014.easttroutlake01.R1.

Yoshida, Y., and H. Oshio, 2022: GOSAT-2 TANSO-FTS-2 SWIR L2 Retrieval Algorithm Theoretical Basis Document. (Available online at: https://prdct.gosat-2.nies.go.jp/documents/pdf/ATBD_FTS-2_L2_SWL2_en_01.pdf, accessed 9 March 2023)

Yoshida, Y., N. Kikuchi, I. Morino, O. Uchino, S. Oshchepkov, A. Bril, T. Saeki, N. Schutgens, G. C. Toon, D. Wunch, C. M. Roehl, P. O. Wennberg, D. W. T. Griffith, N. M. Deutscher, T. Warneke, J. Notholt, J. Robinson, V. Sherlock, B. Connor, M. Rettinger, R. Sussmann, P. Ahonen, P. Heikkinen, E. Kyrö, J. Mendonca, K. Strong, F. Hase, S. Dohe, and T. Yokota, 2013: Improvement of the retrieval algorithm for GOSAT SWIR XCO_2 and XCH_4 and their validation using TCCON data. *Atmos. Meas. Tech.*, **6**, 1533–1547, doi:10.5194/amt-6-1533-2013.

Yoshida, Y., N. Eguchi, Y. Ota, N. Kikuchi, K. Nobuta, T. Aoki, and T. Yokota, 2017: Algorithm theoretical basis document (ATBD) for CO_2, CH_4 and H_2O column amounts retrieval from GOSAT TANSO-FTS SWIR. (Available online at: https://data2.gosat.nies.go.jp/doc/documents/ATBD_FTSSWIRL2_V2.0_en.pdf, accessed 18 May 2023)